The Muon $g-2$ experiment at Fermilab and the First Physics Run

Dikai Li[*][†]

Shanghai Jiao Tong University
China University of Geosciences
E-mail: dikai.li@sjtu.edu.cn

Measurement of the muon anomalous magnetic moment (muon g-2) is a sensitive tool for testing the Standard Model (SM) and searching for new physics. It is an important and complementary tool to probe the high energy frontier. In this talk, I will provide an overview on the Fermilab Muon g-2 experiment, which aims to perform the measurement the muon g-2 with a precision goal of 140 parts per billion, a fourfold improvement over the previous BNL measurement. The first physics run finished in 2018 collecting a data sample with similar size of the BNL measurement. The current experimental status and prospects of the experiment will also be discussed.

PoS(LATTICE2019)258

---

[*]Speaker.

1. Introduction

The particle's magnetic moment is related to its intrinsic spin by the Lande $g-$factor or gyro-magnetic ratio[1]:

$$\vec{u} = g\frac{q}{2m}\vec{S}. \tag{1.1}$$

In general, different particles have different $g-$factors. For structureless spin-1/2 particles, particularly electrons and muons, Dirac's equation suggests g equals 2 if no quantum corrections are considered[2]. Due to quantum corrections, the $g-$factor deviates from 2[3]. The extent to which g differs from 2 is called the anomalous magnetic moment and defined as

$$a \equiv \frac{g-2}{2} \tag{1.2}$$

. The anomaly arising comes from leading-order QED correction is

$$a = \frac{\alpha}{2\pi} \tag{1.3}$$

, which was presented first by Julian Schwinger in 1948[4]. Three components of the Standard Model account for such anomalous magnetic moment of the muon:

$$a_\mu^{\text{SM}} = a_\mu^{\text{QED}} + a_\mu^{\text{EW}} + a_\mu^{\text{Had}} \tag{1.4}$$

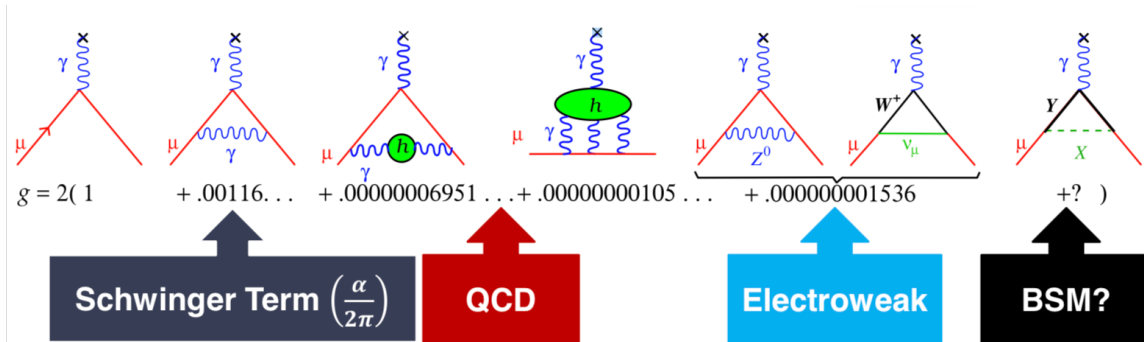, as shown in Figure 1. The recent SM predictions are listed in Table 1.

Figure 1: Feynman diagrams contributing to muon $g - 2$

From the experimental aspect, a_μ was measured most recently in 2006 with a precision of 540 parts per billion (ppb) at Brookhaven National Lab (E821) [12]. The current value of a_μ^{exp} is [13]

$$a_\mu^{\text{exp}} = (11659208.9 \pm 6.3) \times 10^{-10} \tag{1.5}$$

. With the value determined by Keshavarzi et al.[7]

$$a_\mu^{\text{exp}} - a_\mu^{\text{SM}} = (26.86 \pm 7.24) \times 10^{-10} \tag{1.6}$$

, corresponds to a nonzero difference between E821's measurement and the Standard Model prediction with a significance of 3.7σ. See Figure 2 for a visual comparison between SM prediction and the experimental measurement. The Muon $g - 2$ Experiment at Fermilab (E989)[14] is aiming at reducing the experimental uncertainty down to 140 ppb, a factor-of-4 improvement from E821, which will give 7.0σ discrepancy from SM prediction if both center values from SM and experiment aspects stay as current.

Contribution	a_μ value ($\times 10^{-10}$)
QED[5] (Tenth-order)	11658471.895±0.008
Hadronic VP (LO) [DHMZ-17][6]	693.1±3.4
Hadronic VP (LO) [KNT-18][7]	693.3±2.5
Hadronic VP (NLO) [DHMZ-17]	-9.87±0.07
Hadronic VP (NLO) [KNT-18]	-9.82±0.04
Hadronic VP (NNLO)[8]	1.24±0.01
Hadronic LbL (LO+NLO)[9, 10]	10.1±2.6
Electroweak[11]	15.36±0.10
Total SM [DHMZ-17]	11659181.8±4.3
Total SM [KNT-18]	11659182.1±3.6

Table 1: SM contributions to muon $g − 2$

2. The E989 Muon $g − 2$ Experiment

In E989, a polarized muon beam is stored in a storage ring with a uniform magnetic field, then the point like particle, muon, with spin, mass *m* and charge *e* will follow a circular path in the plane defined by the magnetic field, and its spin direction will rotate in the same plane. The muon's circular motion is called cyclotron motion and its spin rotation is called spin precession. The difference between muon's cyclotron angular frequency and its spin precession angular frequency is called the anomalous precession frequency, $\vec{\omega}_a$, and defined as[1]

$$
\begin{aligned}
\vec{\omega}_a &= \vec{\omega}_s - \vec{\omega}_c \\
&= [-\frac{ge\vec{B}}{2m} - (1-\gamma)\frac{e\vec{B}}{m\gamma}] - [-\frac{e\vec{B}}{m\gamma}] \\
&= -(\frac{g-2}{2})\frac{e\vec{B}}{m} \\
&= -a\frac{e\vec{B}}{m},
\end{aligned}
\tag{2.1}
$$

where ω_s is the spin precession angular frequency, ω_c is the orbital angular frequency (cyclotron frequency), γ is the relativistic Lorentz factor, g is the particle's $g−$factor, $\vec{B}$ is the magnetic fields experienced by he muon, and a is the anomalous magnetic moment of muon. So one can measure $g − 2$ through observing the anomalous precession frequency and the magnetic field.

The magnetic field in the muon storage region is mapped using proton Nuclear Magnetic Resonance (NMR) probes, which measures the free, non-relativistic proton Larmor precession angular frequency ω_p. Then the magnetic field could be expressed as

$$
B = \frac{\hbar\omega_p}{2\mu_p},
\tag{2.2}
$$

where μ_p is the proton's magnetic dipole moment. And considering the electron's magnetic dipole moment μ_e,
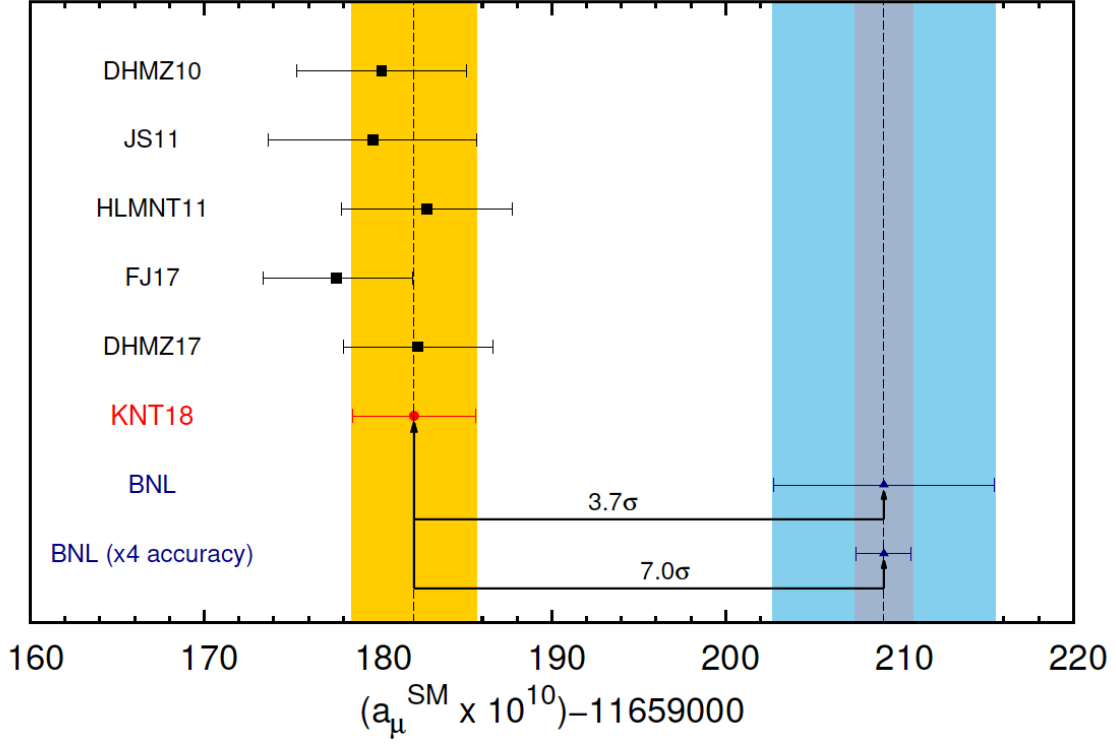
$$
\mu_e = g_e\frac{eS_e}{2m_e},
\tag{2.3}
$$

Figure 2: Comparison between recent SM calculations of the anomalous magnetic moment of muon a_μ and the E821 result. The "BNL($\times 4$) accuracy" point represents the projected uncertainty of E989. This figure was originally presented in Reference[7])

where $S_e = \frac{\hbar}{2}$ is the electron's spin, g_e and m_e are electron's $g-$factor and mass respectively, so

$$e = \frac{4m_e\mu_e}{\hbar g_e}, \tag{2.4}$$

Replace magnetic field and charge in equation 2.1 using equations 2.2 and 2.4, then yields the following relation:

$$a_\mu = \frac{g_e}{2}\frac{\omega_a}{\omega_p}\frac{m_\mu}{m_e}\frac{\mu_p}{\mu_e} \tag{2.5}$$

Considering the nonuniformities in the magnetic field, the quantity ω_p should be replaced with $\tilde{\omega}_p$, where $\tilde{\omega}_p$ is the particle distribution weighted spatial average of the proton Larmor precession frequency. Then the equation reads

$$a_\mu = \frac{g_e}{2}\frac{\omega_a}{\tilde{\omega}_p}\frac{m_\mu}{m_e}\frac{\mu_p}{\mu_e} \tag{2.6}$$

, where ω_a and $\tilde{\omega}_p$ are measured in the E989 storage ring, whereas the $g-$factor of an electron g_e, muon-to-electron mass ratio m_μ/m_e, and proton-to-electron magnetic moment ratio μ_p/μ_e have been already measured with uncertainties better than 22 ppb[13].

Muons are unstable particles and predominantly decay into a positron and two neutrinos

$$\mu^+ \rightarrow e^+ \nu_e \bar{\nu}_\mu. \tag{2.7}$$

3

Muon decay proceeds through the weak interaction and therefore exhibits parity violation, and such parity violation causes the correlation between the decay positron momentum and the muon spin is nonzero. Consequently the positron energy E distribution is [14]

$$\frac{\mathrm{d}P}{\mathrm{d}E} = N(E)[1 + A(E)\cos\alpha], \tag{2.8}$$

where $N(E)$ describe the lab frame energy distribution,A_E is called the asymmetry and encodes how strong the correlation between the positron momentum and muon spin, α is the angle between the muon and its momentum. Figure 3 shows the muon decay energy distribution, when the spin and momentum are aligned, the decay positron energy distribution shifts in favor of higher energies. Since the rate of change of α is exactly ω_a, replacing α with $\omega_a t + \phi$ yields the positron energy
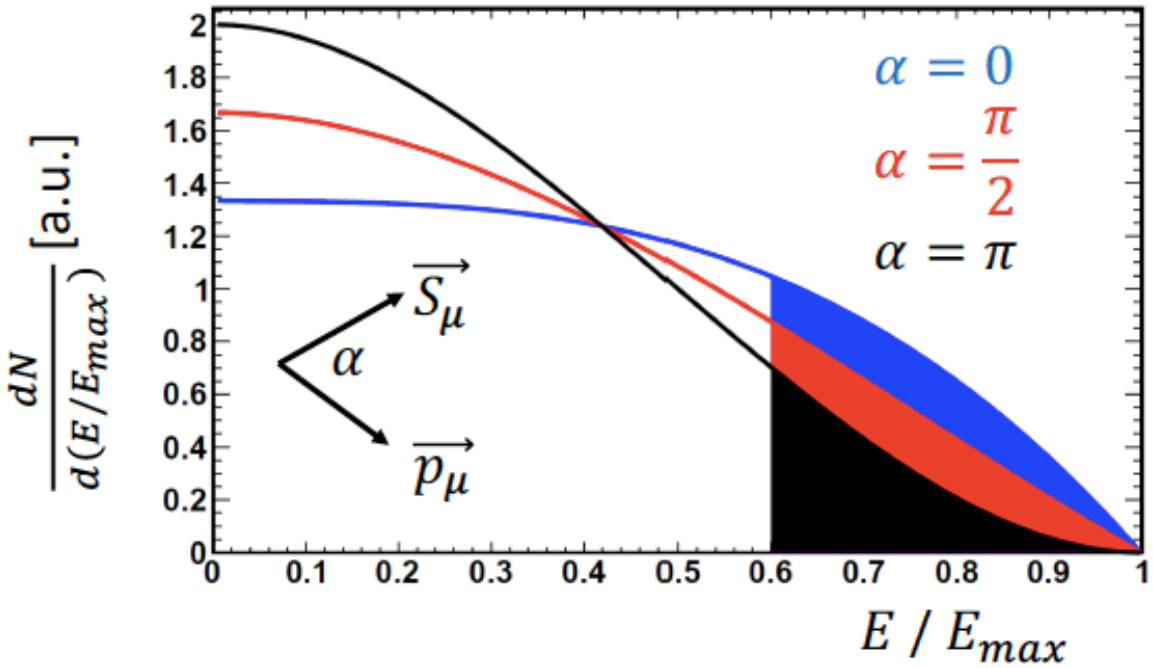

Figure 3: Muon decay energy distribution in the lab frame for three different values of the angle between the muon spin and its momentum, α.[15])

distribution as

$$\frac{\mathrm{d}^2 P}{\mathrm{d}E\mathrm{d}t} \propto e^{-t/(\gamma\tau_\mu)}N(E)[1 + A(E)\cos(\omega_a t + \phi)] \tag{2.9}$$

There are 24 electromagnetic calorimeters stationed around the inner radius of the storage ring. When a muon decays, the produced decay positron has less energy than its parent muon and correspondingly a smaller orbit radius in the storage ring's magnetic field; decay positrons curl toward the center of the ring and hit the crystals of the calorimeters.

The calorimeter would record the signals which represent the decay positron hit energy and time. An analysis technique called the T-method or threshold method, gives weight 1 to positrons above a certain energy threshold and 0 to positrons below that threshold. Then all signals in a number of threshold are summed up to yield a one dimensional T-Method histogram. Figure 2.9

illustrates how a T-Method histogram is constructed. Then equation 2.9 suggests the fit model:

$$N(t) = N_0 e^{-t/\tau}[1 + A\cos(\omega_a t + \phi)], \tag{2.10}$$

where N is the overall normalization, τ is the boosted muon lifetime, A is the overall asymmetry, ϕ is the initial phase, ω_a is the anomalous precession frequency.

Besides T-Method, E989 analysis groups adopt various approaches extracting ω_a. For example the energy binned analysis, in which doesn't sum up all the different energy windows, otherwise each of the sub histogram is fit separately using the fitting function getting $\omega_{a,E}$, and the the $\omega_{a,E}$'s can be averaged to obtain a single combined value $\langle \omega_a \rangle$.

Other approach like E-weighted is similar to T-Method, the only difference is just giving the positron above E-threshold with weight equals the positron energy but not with weight 1.

There are three key steps to achieve a 140 ppb measurement at Fermilab E989: 3 times more uniform magnetic field that aims at reducing the ω_p systematic uncertainty from 170 to 70 ppb, improved instrumentation for ω_a measurement that aims at reducing the ω_a systematic uncertainty from 180 to 70 ppb, and 21 times more decay positrons than BNL E821 that aims at reducing the ω_a statistical uncertainty from 460 to 100 ppb.

At Fermilab short batches of 8 GeV protons are injected into Recycler Ring, each batch is split into 4 bunches of 10^{12} protons, then bunch is extracted one by one to hit target to produce pion. A long beam line is used to collect the muon decay from pion. Then the beam with protons, pions and muons enter the Delivery Ring, where pions decay away, protons are aborted, and muons are extracted and transfered to Muon $g − 2$ storage ring. Such muon beam injection is 4 times higher fill frequency than BNL.

At the point the injected muon beam connected to the storage ring, an inflector magnet is used to proved field free region to deliver beam to the edge of the storage region, and also to stop strong deflection of the beam.

Since the incident of muon beam center is 77 mm off from the center of the storage ring, 3 kicker magnets are placed to provide 10.8 mrad "kick" to put muons onto the storage orbit.

Electrostatic quadrupoles are placed in the storage ring to focus muon beam vertically. And such an electric field perpendicular to a muon's momentum affects the muon's spin precession frequency[14],

$$\vec{\omega}_a = -\frac{e}{m}[a_\mu \vec{B} - (a_\mu - \frac{1}{\gamma^2 - 1})\frac{\vec{\beta} \times \vec{E}}{c}]. \tag{2.11}$$

For a proper choice of γ, the effect of the electric field on the anomalous precession frequency will become very small. With a so-called magic γ of 29.3 corresponds to a muon momentum of 3.094 GeV/c, then equation 2.11 would become equation 2.1

3. Physics Run 1 Analysis Progress

E989 physics run 1 data taking period was from April to July 2018, and accumulated about 1.3 times BNL statistics (after data quality cuts), corresponded to 350 ppb statistical uncertainty of ω_a. Meanwhile the magnetic field uniformity was 2 times better than BNL.

From the decay positron hit energy and time information recorded by calorimeter, a two dimensional E-T "raw histogram" could be constructed. Then main systematic uncertainties effects

would be considered, for example the in-fill gain stability, pileup events, lost muons, beam motion and so on. After that a one dimensional time "final histogram" for specific energy muons, chosen according to analysis approach, would be produced. Finally fitting the histogram with model function would extract ω_a.

Figure 4 illustrate a typical 2D decay positron energy v.s. time histogram. Such 2D histogram will be divided into separate energy slices, as shown in figure 5, and in T-Method the energy slices above a certain energy threshold would be summed up as the following equation:

$$A_1 \cos(\omega t + \phi_1) + A_2 \cos(\omega t + \phi_2) = A_3 \cos(\omega t + \phi_3). \tag{3.1}$$

Since in each energy slice the asymmetry A_i and phase ϕ_i is different, improper energy slice divide would affect the ω fitting result. Gain instability would reduce energy slice. Pileup means more than one low energy hit could be misidentified as one high energy hit, as shown in Figure 6, so this will makes additional energy slices are summed up.
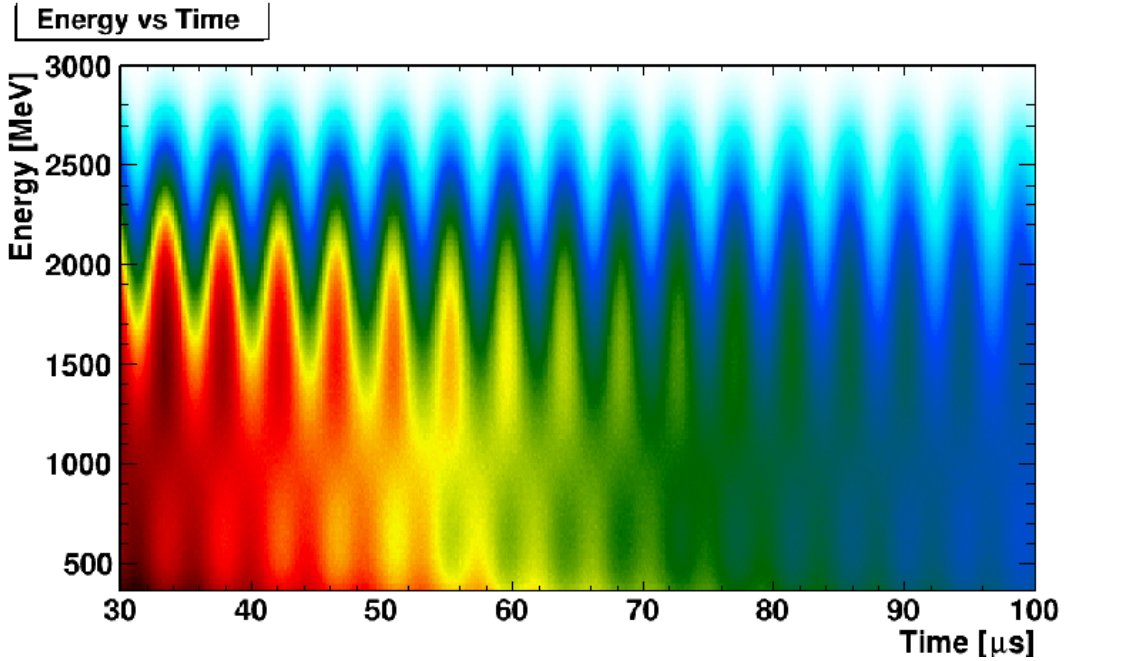

Figure 4: 2D energy v.s. time histogram of decay positron

The above mentioned gain and pileup effects are called detector effects. Besides that there are beam dynamics effects. For example some muons do not decay while flying around the storage ring and hit the calorimeter directly, these are called muon losses, as shown in Figure 7. In this case, muon will penetrate more than one calorimeter in a relatively short time interval, so a coincidence algorithm is used to catch the hit such muon losses, and this will provide an additional factor on the fitting function[16]:

$$\Lambda(t) = 1 - K_{loss} \int_0^t e^{t'/\tau} L(t') \mathrm{d}t', \tag{3.2}$$

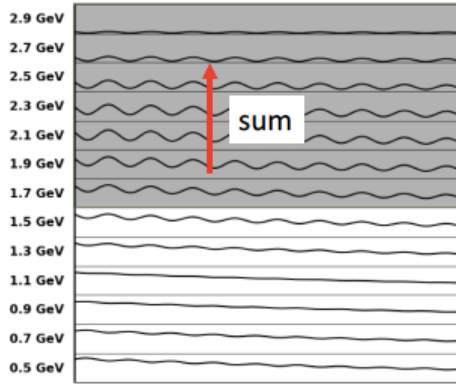where $L(t')$ is the muon loss coincidence function.

6

Figure 5: The 2D energy v.s. time histogram is divided into separate energy slices, and the slices above the energy threshold will be summed up for T-Method.
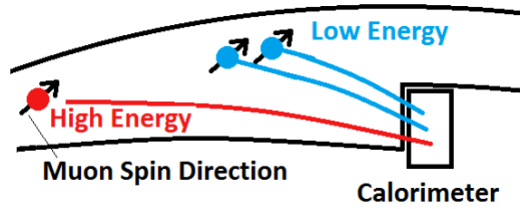

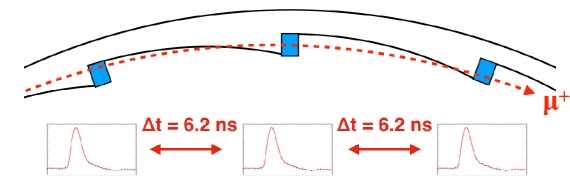**Figure 6:** Illustration of pile-up

Figure 7: Illustration of muon loss

Another main beam dynamics effect is called Coherent Betatron Oscillation (CBO), corresponds to the difference between the cyclotron frequency and the betatron frequency, as shown in Figure 8. And the CBO effect needs to be taken into consideration while fitting[15]:

$$C(t) = 1 - e^{-t/\tau_{cbo}} A_1 \cos(\omega_{cbo} t + \phi_1) \tag{3.3}$$

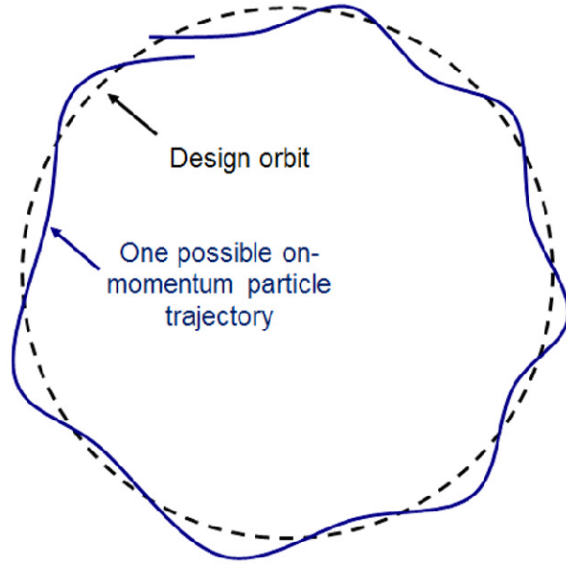After considering all the detector and beam dynamics effects, the final 20 parameters fit func-

Figure 8: Illustration of Coherent Betatron Oscillation

tion:

$$N = N_0 \Lambda N_{cbo} N_{2cbo} N_{VW} e^{-t/\tau} (1 - AA_{cbo} \cos(\omega_a t + \phi\phi_{cbo}))$$

$$N_{cbo} = 1 - A_{1cbo} e^{-\frac{t}{\tau_{cbo}}} \cos(\omega_{cbo} t + \phi_{1cbo})$$

$$N_{2cbo} = 1 - A_{2cbo} e^{-\frac{t}{2\tau_{cbo}}} \cos(2\omega_{cbo} t + \phi_{2cbo})$$

$$N_{VW} = 1 - A_{VW} e^{-\frac{t}{\tau_{VW}}} \cos(\omega_{VW} t + \phi_{VW})$$

$$A_{cbo} = 1 - A_{Acbo} e^{-\frac{t}{\tau_{cbo}}} \cos(\omega_{cbo} t + \phi_{Acbo})$$

$$\phi_{cbo} = 1 - A_{\phi cbo} e^{-\frac{t}{\tau_{cbo}}} \cos(\omega_{cbo} t + \phi_{\phi cbo})$$

$$\omega_{cbo} = \omega_0 (1 + 2.875 e^{-\frac{t}{76}} / \omega_0 t + 5.47 e^{-\frac{t}{8.85}} / \omega_0 t)$$

$$\Lambda = 1 - K_{loss} \int L(t') e^{t'/64.4} \mathrm{dt}, \qquad\qquad (3.4)$$

The fitting result is shown in Figure 9[17].

One important thing needs to be emphasized here is that the analysis is double blinded: the E989 clock is detuned from the nominal frequency of 40 MHz to some 39.xx MHz; and the fitting procedure comes with a random offset in frequency about ω_a to $\omega_a \pm 25$ ppm. So the reader needs to caution this while interpreting the $\omega_a$numbers from figure 9.

Also there are 6 independent analyses were blinded from each other, on Feb 26, 2019 a relative unblinding is performed. Figure 10 shows comparison among 6 independent analyses. The left one in Figure 10 is the result of ω_a randomly blinded, the right one in figure 10 shows the result while all 6 independent analyses commonly using a same blinding phrase. From the zoomed in figure of the commonly blinding result, 6 independent analyses are consistent to each other, and the systematic uncertainties is within 2 ppm[18].

Actually the data analysis is currently ongoing, till the date of the proceeding submitted in November (around E989 Nov-collaboration meeting), Shanghai Jiao Tong University analysis
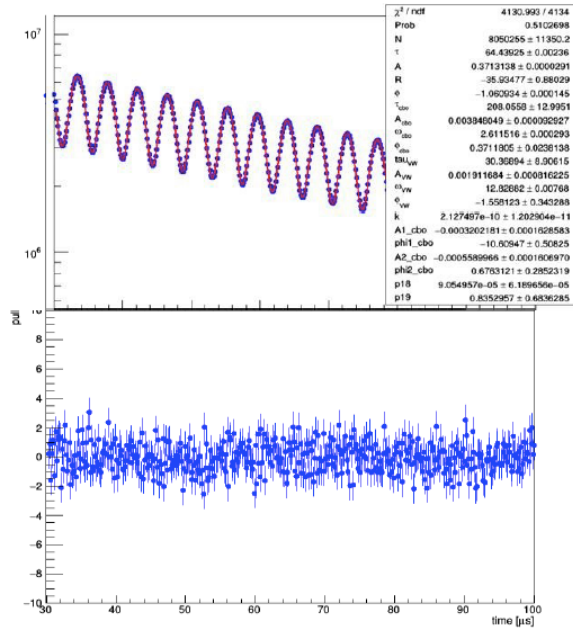
Figure 9: Fitting the decay positron 1D time histogram using 20-parameter function
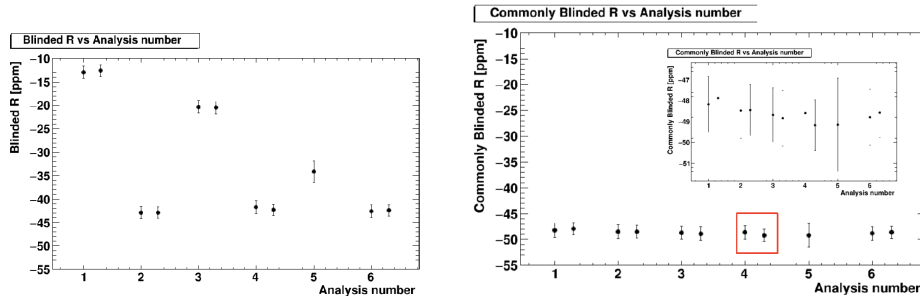

Figure 10: Blinded ω_a results among 6 independent analyses

group's ω_a systematic uncertainty is reduced to 0.88 ppm.

4. Conclusion

The persisting larger than 3σ between SM prediction and experiment measurement in muon anomalous magnetic moment has called for improved precision in both theoretical prediction and measurement. The Fermilab Muon $g − 2$ E989 aims to improve the precision by a factor of 4 in the next few years, this will give 7σ discrepancy assuming both theoretical and experimental central values unchanged. Physics Run 1 of E989 was completed in 2018, and accumulated around 1.3 times BNL statistics. With only run 1 data combined with BNL result, it will provide larger than 5σ discrepancy, assuming central values unchanged. A relative of partial Run 1 data for ω_a analysis has been performed, all 6 independent analyses is consistent with each other.

Run 2 started production running in late March 2019, it's recording about 4 percent of BNL statistics per day, and aims to accumulate 2 times of BNL statistics. Run 3 is projecting about 10

times of BNL statistics. The result on whole Run 1 dataset is still tuned, projected to be announced in the near future.

References

[1] John David Jackson, *Classical electrodynamics*, Wiley India, 2011.

[2] P. A. M. Dirac. The Quantum Theory of the Electron. *Proceedings of the Royal Society of London Series A*, 117:610-624, February 1928.

[3] J. E. Nafe, E. B. Nelson and I. I. Rabi, *Phys. Rev.* 71, 914, 1947

[4] Julian Schwinger, On quantum-electrodynamics and the magnetic moment of the electron, *Phys. Rev.* 73, 416-417, Feb 1948

[5] Tatsumi Aoyama, Masashi Hayakawa, Toichiro Kinoshita, and Makiko Nio, Complete Tenth-Order QED Contribution to the Muon $g − 2$, *Phys. Rev. Lett.*, 109, 111808, 2012

[6] Michel Davier, Andreas Hoecker, Bogdan Malaescu, Zhiqing Zhang, Reevaluation of the hadronic vacuum polarisation contributions to the Standard Model predictions of the muon g-2 and alpha(mZ) using newest hadronic cross-section data, *Eur. Phys. J. C* 77, 827, 2017

[7] Alexander Keshavarzi, Daisuke Nomura, and Thomas Teubner, Muon $g − 2$ and $\alpha(M_z^2)$, A new data-based analysis, *Phys. Rev. D*, 97, 114025, 2018

[8] Alexander Kurz, Tao Liu, Peter Marquard, Matthias Steinhauser, Hadronic contribution to the muon anomalous magnetic moment to next-to-next-to-leading order, *Phys. Lett. B*, 734, 144, 2014

[9] Gilberto Colangelo, Martin Hoferichter, Andreas Nyffeler, Massimo Passera, Peter Stoffer, Remarks on higher-order hadronic corrections to the muon $g − 2$, *Phys. Lett. B*, 735, 90, 2014

[10] Fred Jegerlehner, Leading-order hadronic contribution to the electron and muon $g − 2$, *EPJ Web of Conferences*, 118, 01016, 2016

[11] C. Gnendiger, D. Stöckinger, and H. Stöckinger-Kim, The electroweak contributions to $(g − 2)_\mu$ after the Higgs-boson mass measurement, *Phys. Rev. D*, 88, 053005, 2013

[12] G. W. Bennett et al. Final Report of the Muon E821 Anomalous Magnetic Moment Measurement at BNL. *Phys. Rev., D* 73:072003, 2006.

[13] Peter J. Mohr, David B. Newell, and Barry N. Taylor. CODATA recommended values of the fundamental physical constants: 2014. *Rev. Mod. Phys.*, 88:035009, Sep 2016.

[14] J. Grange et al. Muon $(g − 2)$ Technical Design Report, 2015.

[15] Aaron T. Fienberg, Measuring the Precession Frequency in the E989 Muon $g − 2$ Experiment, Ph.D. thesis, 2019

[16] Jason Crnkovic, Sudeshna Ganguly, William Morse, and Diktys Stratakis. Lost Muon Study for the Muon g-2 Experiment at Fermilab. In *Proceedings, 8th International Particle Accelerator Conference (IPAC 2017): Copenhagen, Denmark, May 14-19, 2017*, page WEPIK119, 2017.

[17] Zhaolin Chu, Bingzhi li, Dikai Li, Liang Li, E989 Note 16312: SJTU Analysis Note for 60h Dataset Relative Unblinding, 2019

[18] Kim Siang Khaw, E989 NOTE 16667: Notebook and plots for the 60h relative unblinding ceremony, 2019

PoS(LATTICE2019)258